Sekiguchi, K., & Hakomori, S. (1983) *Biochemistry 22*, 1415–1422.
Sekiguchi, K., Hakomori, S., Funahashi, M., Matsumoto, I., & Seno, N. (1983) *J. Biol. Chem. 258*, 14359–14365.
Skorstengaard, K., Thögersen, H. C., & Petersen, T. E. (1984) *Eur. J. Biochem. 140*, 235–243.
Stamataglou, S. C., & Keller, J. M. (1982) *Biochim. Biophys. Acta 719*, 90–97.
Stemberger, A., & Hörmann, H. (1976) *Hoppe Seyler's Z. Physiol. Chem. 357*, 1003–1005.
Tooney, N. M., Amrani, D. L., Homandberg, G. A., McDonald, J. A., & Mosesson, M. W. (1982) *Biochem. Biophys. Res. Commun. 108*, 1085–1091.
Wasteson, Å, Wastermark, B., Lindahl, U., & Ponten, J. (1972) *Int. J. Cancer 12*, 169–178.
Welsh, E. J., Frangou, S. A., Morris, E. R., Rees, D. A., & Chavin, S. I. (1983) *Biopolymers 22*, 821–831.
Wessler, E. (1968) *Anal. Biochem. 26*, 439–444.
Venyaminov, S. Y., Metsis, M. L., Chernousov, M. A., & Koteliansky, V. E. (1983) *Eur. J. Biochem. 135*, 485–489.
Vuento, M. (1979) *Hoppe Seyler's Z. Physiol. Chem. 360*, 1327–1333.
Vuento, M., & Vaheri, A. (1979) *Biochem. J. 183*, 331–337.
Vuento, M., Wrann, M., & Ruoslahti, E. (1977) *FEBS Lett. 82*, 227–231.
Yamada, K. M. (1982) *The Glycoconjugates*, Vol 3, pp 331–363, Academic Press, New York.
Yamada, K. M., & Kennedy, D. W. (1979) *J. Cell Biol. 80*, 492–498.
Yamada, K. M., Yamada, S. S., & Pastan, I. (1975) *Proc. Natl. Acad. Sci. U.S.A. 72*, 3158–3162.
Yamada, K. M., Kennedy, D. W., Kimata, K., & Pratt, R. M. (1983) *J. Biol. Chem. 255*, 6055–6063.
Zardi, L., Siri, A., Carnemolla, B., Santi, L., Gardner, W. D., & Hoch, S. O. (1979) *Cell (Cambridge, Mass.) 18*, 649–657.

Nanosecond Optical Spectra of Iron–Cobalt Hybrid Hemoglobins: Geminate Recombination, Conformational Changes, and Intersubunit Communication†

James Hofrichter,*,‡ Eric R. Henry,‡ Joseph H. Sommer,‡,§ Robert Deutsch,‡ Masao Ikeda-Saito,‖ Takashi Yonetani,‖ and William A. Eaton‡

Laboratory of Chemical Physics, National Institute of Arthritis, Diabetes, and Digestive and Kidney Diseases, National Institutes of Health, Bethesda, Maryland 20205, and Department of Biochemistry and Biophysics, University of Pennsylvania School of Medicine, Philadelphia, Pennsylvania 19104

Received July 30, 1984

ABSTRACT: Hybrid hemoglobins were prepared in which cobalt was substituted for the heme iron in either the α or β subunits. Transient optical absorption spectra were measured at room temperature for these hybrids at time intervals between 0 and 50 ms following photodissociation of the carbon monoxide complex with 10-ns laser pulses. The cobalt porphyrins do not bind carbon monoxide, making it possible to investigate the time-resolved response of the cobalt-containing subunits to photodissociation of carbon monoxide in the iron-containing subunits. At the same time the response of the iron-containing subunits to the photolysis event can be studied, permitting an independent determination of the kinetics of ligand rebinding and conformational changes in the α and β subunits of an intact tetramer. The data were analyzed by using singular-value decomposition to obtain the kinetic progress curve for ligand rebinding, the deoxyheme and cobalt porphyrin spectral changes, and the time course of these spectral changes. The geminate rebinding kinetics following photodissociation of $\alpha(Co)_2\beta(Fe\text{-}CO)_2$ were very similar to those found for unsubstituted hemoglobin, $\alpha(Fe\text{-}CO)_2\beta(Fe\text{-}CO)_2$, indicating equivalence of the geminate kinetics for α and β subunits within the R-state tetramer. The results for $\alpha(Fe\text{-}CO)_2\beta(Co)_2$ were consistent with this conclusion, even though the analysis was complicated by the presence of comparable populations of R- and T-state species. Comparison of the deoxyheme spectral changes and relaxation times among the three molecules indicated that both α and β subunits contribute to the deoxyheme spectral changes that signal tertiary and quaternary conformational changes in the unsubstituted tetramer. The response of the cobalt porphyrins to photodissociation was similar in the two hybrids. No structural changes were detected in the cobalt-containing subunits until the second tertiary conformational change in the iron-containing subunits observed at 1–2 μs. Much larger structural changes, as judged by the amplitude of the spectral changes, occurred in the cobalt-containing subunits concomitant with the R $\rightarrow$ T quaternary change at about 20 μs.

Since the introduction of time-resolved absorption and Raman spectroscopy using picosecond and nanosecond lasers, there have been a number of studies on the photodissociation of oxygen and carbon monoxide from hemoglobin (Hb) [see papers in Ho et al. (1982) and reviews by Friedman et al. (1982) and Noe (1982)]. A major objective of these investigations has been to develop a detailed description of the processes occurring subsequent to photodissociation and to relate these processes to the mechanism for the overall thermal dissociation and binding reactions. In particular, one would like to know the rates of the various conformational changes that are known to take place from X-ray diffraction studies

† Work done at the University of Pennsylvania was supported by Research Grants HL14508 (T.Y.) and AI20463 (M.I.-S.) from the National Institutes of Health and Grant PCM7316835 (T.Y.) from the National Science Foundation.
‡ National Institutes of Health.
§ Present address: Department of Physics and Astronomy, University of Rochester, Rochester, NY 14627.
‖ University of Pennsylvania School of Medicine.

0006-2960/85/0424-2667$01.50/0

(Perutz, 1970; Baldwin & Chothia, 1979) and how these conformational changes are related to ligand rebinding and the motion of the ligand in the protein. We have been investigating this problem by measuring optical absorption spectra in the Soret region (400–460 nm) with high precision following photodissociation of (carbonmonoxy)hemoglobin (HbCO) with 10-ns laser pulses (Hofrichter et al., 1983; Henry et al., 1984). Measurement of precise spectra permits the acquisition of kinetic data for conformational changes, which produce only small changes in the heme absorption spectra, as well as for ligand rebinding.

Following complete photodissociation of HbCO at room temperature, five relaxations are observed (Hofrichter et al., 1983). The first relaxation at about 50 ns (which we call relaxation I) corresponds to rebinding of the photodissociated molecule that has not yet escaped into the solvent, i.e., geminate recombination (Duddell et al., 1979; Alpert et al., 1979; Friedman & Lyons, 1980; Lindqvist et al., 1981; Catterall et al., 1982; Hofrichter et al., 1983). Associated with this relaxation is a change in the deoxyheme spectrum signaling some kind of conformational change (Hofrichter et al., 1983). The second and third relaxations (called relaxations II and III), occurring at about 1 and 20 μs, are primarily deoxyheme spectral relaxations, with a small amount of associated ligand rebinding. Deoxyheme spectral changes in this time regime have also been observed by resonance Raman spectroscopy (Lyons & Friedman, 1982). On the basis of partial photolysis experiments the 20-μs relaxation (relaxation III) has been assigned to the R $\rightarrow$ T quaternary change of zero-liganded molecules (Hofrichter et al., 1983). The 50-ns and 1-μs changes in the deoxyheme spectra correspond, therefore, to tertiary conformational changes within the R quaternary structure (Hofrichter et al., 1983). The remaining two relaxations (IV and V) are dependent on the CO concentration and result from bimolecular rebinding to molecules in the R and T quaternary conformations, respectively (Sawicki & Gibson, 1976; Hofrichter et al., 1983).

Because the spectra of the hemes in the α and β subunits are indistinguishable in these experiments, their relative contributions to the geminate recombination and deoxyheme spectral changes are not known. In order to study the kinetics of ligand rebinding and conformational changes in the individual subunits within the tetramer, we have begun an investigation of iron–cobalt hybrid hemoglobin molecules. In these molecules cobalt(II) is substituted for iron(II) in either the α or the β subunits (Ikeda-Saito et al., 1977). X-ray crystallographic studies of hemoglobin in which iron was replaced by cobalt in both α and β subunits showed no change in the globin conformation (Fermi et al., 1982).[1] The cobalt-substituted molecule binds oxygen cooperatively, but the cooperativity is slightly less than is observed for the iron-containing molecule (Imai et al., 1977). From these X-ray crystallographic and binding studies of the completely cobalt-substituted molecule one would expect the behavior of the individual subunits in the iron–cobalt hybrid molecules to be very close to their behavior in the unsubstituted tetramer.

The iron–cobalt hybrid molecules liganded with CO have two characteristics that make them extremely useful for examining the properties of individual subunits in photolysis experiments (Morris et al., 1984). First, the cobalt porphyrins do not bind CO, so that in the fully saturated $\alpha(\text{Fe-CO})_2\beta(\text{Co})_2$ hybrid CO binds only to the α hemes and in the fully saturated $\alpha(\text{Co})_2\beta(\text{Fe-CO})_2$ hybrid CO binds only to the β hemes (Ikeda-Saito et al., 1977; Ikeda-Saito & Yonetani, 1980). As a result, the response to photodissociation of the α and β subunits within an intact tetramer can be studied independently. Second, the Soret absorption spectrum of the cobalt porphyrins is separated from both the deoxyheme and heme-CO Soret spectra. This permits the observation of the time-resolved response of the cobalt-containing subunits to photodissociation of CO in the iron-containing subunits.

Materials and Methods

Sample Preparation. Human hemoglobin was purified from a lysate by ion-exchange chromatography (Sunshine et al., 1979). The iron–cobalt hybrid hemoglobins were prepared as described previously (Ikeda-Saito et al., 1977). The solutions contained 0.1 M potassium phosphate (pH 7.0) and 0.01 M sodium dithionite to remove any traces of oxygen. The hybrid hemoglobin solutions were equilibrated with CO at 1.0 atm, while the unsubstituted hemoglobin solution was equilibrated with CO at 1.2 atm. Solutions were injected into 0.34-mm path length cuvettes (Wilmad WG-814 EPR flat cells) that had been previously flushed with CO. The cells were sealed with dental wax and varnish (No. 90-8, GC Electronics). The concentrations of hemes were 143 μM for HbCO [i.e., $\alpha(\text{Fe-CO})_2\beta(\text{Fe-CO})_2$], 171 μM for $\alpha(\text{Fe-CO})_2\beta(\text{Co})_2$ (342 μM total porphyrin), and 128 μM for $\alpha(\text{Co})_2\beta(\text{Fe-CO})_2$ (256 μM total porphyrin). The calculation of concentrations was based on a value of 162 500 M^{-1} cm^{-1} per heme for the peak-to-peak difference in the extinction coefficients in the static deoxy-minus-CO difference spectra.

Spectral Measurements. Static spectra were measured with a Cary 17 spectrophotometer interfaced to a Hewlett-Packard 9825 calculator. Processing of the static and transient spectra was carried out on PDP 11/70 and DEC-10 computers.

Transient absorption spectra following complete photodissociation were measured at room temperature (20–22 °C) with a transient laser spectrometer, which has been briefly described previously (Hofrichter et al., 1983; Henry et al., 1983). The spectrometer employs two Nd:YAG lasers. The 532-nm second harmonic output (10-ns pulse, fwhm) of one of these lasers (DCR-1A, Quanta-Ray, Mountain View, CA) is used to photodissociate almost all the molecules in a small slit-shaped region of the sample cuvette. Approximately 4 mJ of laser energy per pulse is incident on the front face of the cuvette. The sample optical density at 532 nm is only about 0.05. This incident power results in about 20 photons absorbed per heme, enough to achieve near-total photodissociation of the sample. The 353-nm third harmonic output of the second laser (Quanta-Ray DCR-1) is cylindrically focused on a cuvette through which a solution (1.2–1.5 mM) of Stilbene 420 dye (Exciton Chemicals, Dayton, OH) in methanol is circulated by a peristaltic pump. The dye provides a reproducible broad-band source with significant emission in the range 395–475 nm. The excited-state population of dye is rapidly depleted by stimulated emission. This forces the temporal profile of the dye pulse to closely follow that of the 10-ns (fwhm) laser pulse.

The slit-shaped dye emission is focused inside the sample cuvette. This image of the source is refocused onto the 100 μm wide entrance slit of a 0.25-m spectrograph with a 600 groove/mm holographic grating (M-20, J-Y Optical Systems, Metuchen, NJ) and dispersed on the face of a silicon vidicon tube (1256E, Princeton Applied Research, Princeton, NJ). A

[1] The lack of a difference was attributed to the identity of the distance between the porphyrin plane and the metal-bonded imidazole nitrogen of the proximal histidine. The displacement of cobalt from the porphyrin plane is smaller than for iron, but the imidazole nitrogen–porphyrin plane distance is unchanged because of a compensating increase in the cobalt–imidazole nitrogen bond length (Fermi et al., 1982).

reference beam is generated by focusing an image of the dye source back onto the dye cuvette, just below the incident laser beam. This image is propagated down the optical train onto the vidicon face, always imaged immediately above or below the dye emission. The main beam goes through an excited region of the sample while the reference beam goes through an unexcited region, so that the optical configuration is that of a double-beam difference spectrometer. The signal is read off the vidicon by an optical multichannel analyzer (OMA II, Princeton Applied Research, Princeton, NJ). The OMA digitizes the intensities from the two tracks, corrects for the dark counts, and calculates the logarithm of the ratio of the intensities to obtain absorption difference spectra that are stored on diskettes pending further analysis. The measured spectra are photolyzed-minus-unphotolyzed difference spectra at various time delays between firing the excitation and probe lasers. Each spectrum is obtained by averaging the results from 36 laser shots, with a minimum delay of 100 ms between each shot.

The time resolution is obtained by delaying the probe laser with respect to the pump laser. The timing pulses are generated by a Hewlett-Packard 5359A time synthesizer, triggered by a 10-Hz clock. The two outputs from the synthesizer are fed into a home-built timing circuit that generates the sequence of pulses required to fire the laser flashlamps and Q switches. The outputs of this timing circuit are, in turn, controlled by a Hewlett-Packard 9826A desktop computer that synchronizes the data acquisition by the OMA with the laser firing sequence and provides a running log of the experiment. The actual delay between laser pulses is measured by using a pair of fast photodiodes (Hewlett-Packard 5082-4220) to trigger a Hewlett-Packard 5335A universal counter. In experiments that require delays greater than 100 ms between the photolysis and probe pulses, the Q-switch outputs of the lasers are blanked by the computer to provide the necessary delay without altering the rate at which the flashlamps are fired.

Data Processing. A single experiment generates 70–110 difference spectra at different time delays between the photolysis and probe laser pulses. Each measured spectrum consists of optical densities at 460 wavelengths but is reduced to 230 wavelengths after five-point cubic smoothing. The spectra are then processed by using singular-value decomposition (Golub & Reinsch, 1970; Shrager & Hendler, 1982; Hofrichter et al., 1983). This procedure transforms the $m \times n$ matrix of data, **A**, consisting of optical densities at m (=230) wavelengths and n (=number of measured spectra) different time delays, into the product of three matrices, i.e., $\mathbf{A} = \mathbf{USV}^T$. **U** is an $m \times n$ matrix consisting of n orthonormal basis spectra; **S** is a diagonal matrix with all nonnegative elements, called the singular values of **A**, which decrease monotonically from the (1,1) element to the (n,n) element; and **V** is an $n \times n$ matrix in which each row of $\mathbf{V}^T$ (column of **V**) is the time course of the amplitude of the corresponding basis spectrum (column of **U**). The singular values are a measure of the contribution of the corresponding basis spectra to the observed spectra. Thus, the first column of **U** (U_1) multiplied by its singular value is the single basis spectrum that, together with the time course of its amplitude, the first column of **V** (V_1), is the best one-component least-squares representation of the data matrix, **A**. Columns 1 and 2 of **U**, multiplied by their singular values and columns 1 and 2 of **V**, are the best two-component least-squares approximation to **A**, and so on. Most of the useful information is contained in the first few components of the singular-value decomposition; the higher components, for the most part, represent noise. The singular-value decomposition (SVD) of the data, therefore, acts as an effective means of improving the signal-to-noise ratio in the spectra.

Basis spectra were chosen to be significant according to three criteria: the magnitude of the singular value, the autocorrelation of the basis spectrum, and the autocorrelation of the time course of the amplitude of the basis spectrum. The autocorrelations of the columns of **U** and **V** were calculated as follows:

$$\mathrm{AC}(U_j) = \sum_{i=1}^{229} U_{ij}U_{i+1,j} \qquad \mathrm{AC}(V_j) = \sum_{i=1}^{n-1} V_{ij}V_{i+1,j} \quad (1)$$

where n is the number of measured spectra. In general, only three of the basis spectra were found to be significant by these criteria. The data set was thus truncated to include only the information contained in these basis spectra and the time course of their amplitudes prior to further processing. The roughly 50 000 data points in a given experiment were thus condensed to approximately 1000 data points by smoothing the SVD analysis.

To proceed further, the selected columns of **V** were fitted to sums of exponentials in order to obtain relaxation times τ_j for the various processes describing the time evolution of the photoproduct, i.e.

$$V_i(t) = \sum_{j=1}^{k} F_{ij}e^{-t/\tau_j} \qquad i = 1, 2, \text{ or } 3 \quad (2)$$

where F_{ij} is the change in the amplitude of the ith basis spectrum accompanying the jth relaxation. In carrying out the fits, we took zero time as the time at which the maximum amplitude was observed in V_1. In the case where the three columns of **V** were fitted to a sum of five exponential relaxations with the same relaxation times, roughly 300 data points were further condensed into a set of 5 rates and 15 values for the F_{ij}, so that the complete result of an experiment is expressed as three basis spectra of 230 points each and 20 parameters that characterize the fits to the time course of the amplitudes of the basis spectra.

The spectrum of the sample prior to a particular relaxation can now be calculated from the basis spectra and amplitudes obtained from the fits to the columns of **V**. The spectrum prior to relaxation k, $D_k(\lambda)$, is given by

$$D_k(\lambda) = \sum_{j=k}^{5} \sum_{i=1}^{3} U_i(\lambda)S_iF_{ij} \quad (3)$$

where $U_i(\lambda)$ is basis spectrum i and S_i is its singular value. To examine spectral changes in the iron-containing subunits other than those resulting from ligand rebinding, it is necessary to compare spectra in which the concentration of deoxyhemes is the same. As a first approximation, these spectra, $N_k(\lambda)$, normalized to the concentration of deoxyhemes in the immediate photoproduct, were calculated from

$$N_k(\lambda) = D_k(\lambda)([\mathrm{Fe}]_1/[\mathrm{Fe}]_k^0) \simeq D_k(\lambda)/(\sum_{j=k}^{5} F_{1j}/\sum_{j=1}^{5} F_{1j}) \quad (4)$$

where $[\mathrm{Fe}]_1$ is the concentration of deoxyhemes at $t = 0$ and $[\mathrm{Fe}]_k^0$ is the concentration of deoxyhemes prior to relaxation k, determined from the fits to V_1. The accuracy of this approximation increases as the magnitude of the spectral change in the photoproduct decreases. A first approximation to the spectral change accompanying each relaxation k was then calculated from the difference spectra $N_{k+1}(\lambda) - N_k(\lambda)$.

Normalization of the measured spectra using the assumption that V_1, summarized by the fit coefficients F_{1j}, reproduces the ligand rebinding is rigorously correct only if the spectra of the

$$\begin{bmatrix} -1 & -1 \\ 1-\alpha & 1 \end{bmatrix} = \begin{bmatrix} (-1-\alpha/4)/\sqrt{2} & (1-\alpha/4)/\sqrt{2} \\ (1-\alpha/4)/\sqrt{2} & (1+\alpha/4)/\sqrt{2} \end{bmatrix} \begin{bmatrix} 2(1-\alpha/4) & 0 \\ 0 & \alpha\sqrt{2}(1+\alpha/4) \end{bmatrix} \begin{bmatrix} (1-\alpha/4)/\sqrt{2} & (1+\alpha/4)/\sqrt{2} \\ (-1-\alpha/4)/\sqrt{2} & (1-\alpha/4)/\sqrt{2} \end{bmatrix} \quad (5)$$

$$A = U \times S \times V^T$$

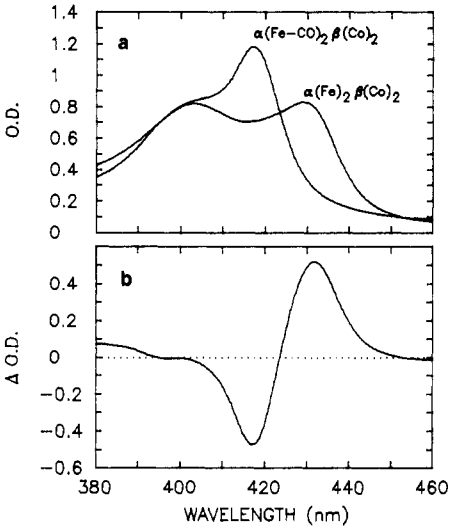

FIGURE 1: Static spectra of $\alpha(Fe)_2\beta(Co)_2$ and $\alpha(Fe\text{-}CO)_2\beta(Co)_2$. (a) Absolute spectra of liganded (171 μM heme, path length = 356 μm) and unliganded hybrid molecules (171 μM heme, path length = 357 μm). (b) Unliganded-minus-liganded difference spectrum.

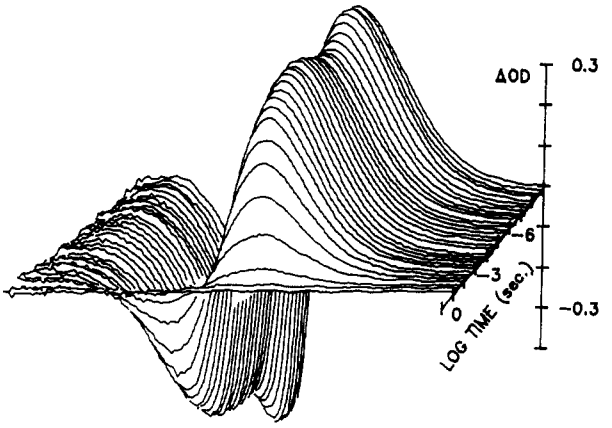

FIGURE 2: Transient spectra of photolyzed $\alpha(Fe\text{-}CO)_2\beta(Co)_2$. One-third of the measured data are displayed as a spectral surface. The spectra are plotted as ΔOD (vertical) vs. wavelength (horizontal). Four spectra per decade are plotted as a function of the logarithm of the time, increasing from 10^{-9} to 10^{-1} s coming foward on the surface. The spectra were smoothed by using a five-point cubic spline fit, and data are plotted at 154 of the measured 460 wavelengths. The wavelength at the extreme left is 394 nm, and that at the extreme right is 460 nm. The increased noise seen at the shortest wavelengths and near the peak of the heme-CO absorption results from the low light intensity of the probe beam in these regions, resulting from self-absorption by the dye and absorption of the liganded hemes, respectively.

deoxy- and CO-hemes are time independent. The physical origin of the problem is most easily understood by considering the case where the spectrum of the photoproduct simply increases in intensity with time. The difference spectrum observed at later times will be larger than that observed at early times if there is no ligand rebinding. As it turns out, the larger difference spectrum produces an increase in the amplitude of the first SVD basis spectrum, equivalent to a decrease in the apparent fractional saturation of the photoproduct (i.e., an apparent dissociation of ligand).

To obtain a first-order correction of the ligand rebinding curve for this effect of spectral changes, we assume that there are no spectral changes of the CO-hemes and that the deoxyheme spectral change is mainly an increase in its extinction coefficient. A simple model calculation treats the heme-CO and deoxyheme spectra as square waves of equal amplitude after the spectral relaxation, but of unequal amplitude prior to the relaxation. If there is no ligand rebinding, the deoxy-minus-CO spectra can be represented as the two-component vectors $(-1, 1-\alpha)$ before the relaxation and $(-1, 1)$ after the relaxation. Singular-value decomposition of these two spectra to first order in α is shown in eq 5. This result shows that the apparent deoxyheme concentration estimated from V_1 increases by a factor of $1 + \alpha/2$ during the relaxation, even though no ligand dissociation has occurred. This calculation suggests that a first-order correction to the ligand rebinding curve can be obtained by renormalizing the estimate of the deoxyheme concentration prior to each relaxation from the fit to V_1 by dividing by the factor $1 - \alpha/2$.

To apply this result to our data, we have used the spectral changes calculated from eq 4 to estimate α_k, the fractional decrease in the deoxyheme extinction coefficient at 430 nm prior to relaxation k, relative to that for equilibrium deoxyhemoglobin, i.e.

$$\alpha_k = [N_5(430) - N_k(430)]/OD_{Fe}(430) \quad (6)$$

where OD_{Fe} is the contribution of the deoxyheme to the optical density at 430 nm for the completely unliganded molecule. As suggested by the model calculations, the deoxyheme concentration prior to each relaxation, $[Fe]_k$, was calculated from the deoxyheme concentration obtained from V_1, $[Fe]_k^0$, from

$$[Fe]_k = [(1-\alpha_1/2)/(1-\alpha_k/2)][Fe]_k^0 \quad (7)$$

The new values of $[Fe]_k$ were used to calculate a new set of normalized spectra from

$$N^*_k(\lambda) = D_k(\lambda)([Fe]_1/[Fe]_k) \quad (8)$$

The renormalized spectra, $N^*_k(\lambda)$, were then used to provide an improved estimate of the α_k's, and the above procedure was iterated until a self-consistent set of $[Fe]_k$'s and renormalized $N^*_k(\lambda)$'s was found. Generally, 5–6 iterations provided a stable solution. This procedure can, in principle, generate an infinite set of ligand rebinding curves and associated spectral changes that differ from the original difference spectra only by the addition or subtraction of a deoxy-minus-CO difference spectrum. On the basis of the analysis of spectral relaxations in which there is no ligand rebinding (see below), we estimate that this "renormalization" procedure is sufficiently accurate to provide the correct ligand rebinding amplitudes (F_{1j}) to within 1% for each relaxation.

RESULTS

Figure 1 shows the static spectra of the $\alpha(Fe)_2\beta(Co)_2$ hybrid with and without CO. The absorption maxima at about 430, 420, and 400–405 nm arise from the deoxyhemes, the CO-hemes, and the cobalt porphyrins, respectively. Figure 2 shows part of the data from a kinetic experiment in which 111 transient spectra were measured at time delays between 0 and 46 ms following photodissociation. Each measured spectrum consisted of optical densities at 460 wavelengths but was reduced to 230 wavelengths after five-point cubic smoothing. The spectra were then processed by using singular-value de-

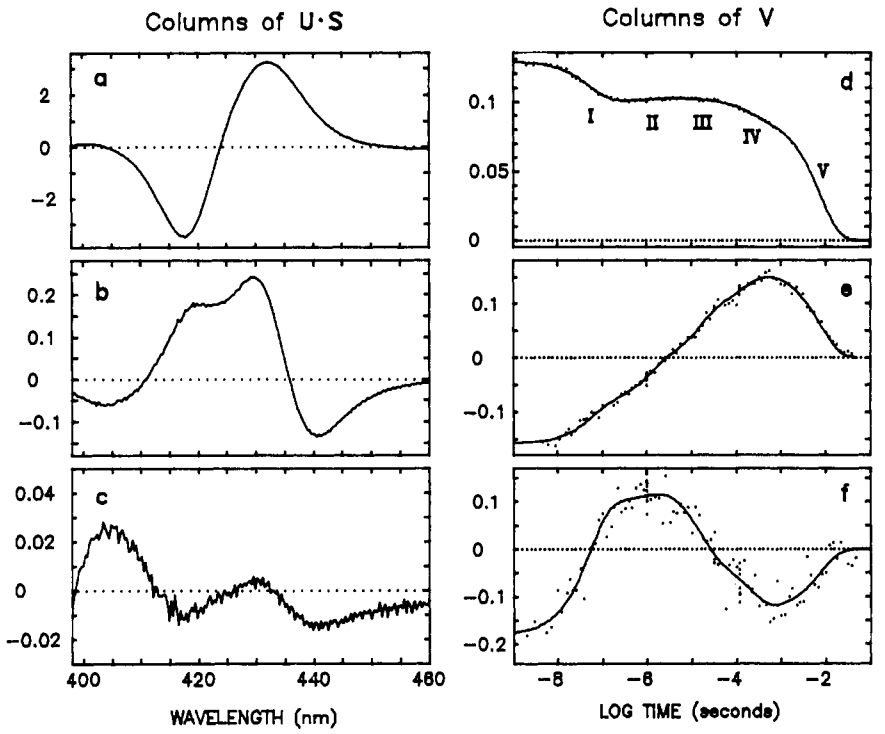

FIGURE 3: Singular-value decomposition of 111 spectra following photodissociation of $\alpha(Fe\text{-}CO)_2\beta(Co)_2$ (sample of Figure 1). Panels a–c are the three significant basis spectra of the U matrix multiplied by their singular values. Panels d–f are the corresponding columns of the V matrix, which give the amplitude of the basis spectra as a function of time. The points are the data, and the solid curves are the results of simultaneous least-squares fits to the data using a sum of five exponentials (eq 2).

composition (see Materials and Methods). For the first six basis spectra the singular values were 23.9, 1.61, 0.41, 0.16, 0.10, and 0.08; the autocorrelations of the corresponding columns of the U matrix were 0.998, 0.998, 0.988, 0.946, 0.674, and −0.296; and the autocorrelations of the corresponding columns of the V matrix were 0.995, 0.967, 0.028, 0.884, 0.455, and 0.119. In the remaining 105 basis spectra the singular values decreased from 0.067 to 0.003; the autocorrelations of the columns of U varied randomly from 0.36 to −0.57; and the autocorrelations of the columns of V varied randomly from 0.21 to −0.27. On the basis of these results, the first, second, and fourth basis spectra were judged to be significant and retained for subsequent analysis. The 108 discarded spectra appeared to represent primarily noise, with contributions from offsets and changes in the shape of the base line. Figure 3 shows the three retained basis spectra (first, second, and fourth columns of U) multiplied by their singular values and the time course of the amplitudes of these basis spectra (first, second, and fourth columns of V). In the following, these spectra will be referred to as basis spectra 1, 2, and 3.

It should be emphasized that these three basis spectra do not represent spectra of molecular species. They are mathematical representations of the data and are required to be orthogonal by the singular-value decomposition. Nevertheless, certain qualitative features are apparent. Basis spectrum 1 with a singular value of 23.9 is mainly a deoxy-minus-CO difference spectrum. Basis spectrum 2 with the next largest singular value of 1.6 is complex, and it appears to contain features resulting from spectral changes of both the cobalt porphyrins and the deoxyhemes, as well as possible contributions from a deoxy-minus-CO spectrum caused by ligand rebinding. Basis spectrum 3 with a singular value of only 0.35 is also complex.

To obtain relaxation times, τ_j, for the various processes, the three columns of V were fit to sums of exponentials according to eq 2. No significant difference was found between the relaxation times and amplitudes obtained by fitting the three columns of V independently and those obtained by fitting all three columns simultaneously with a single set of relaxation times. In the simultaneous fit each column of V was weighted by its singular value. As was found previously with fully photolyzed HbCO (Hofrichter et al., 1983), the data could be adequately fit with five relaxations, labeled I through V. The fitted curves are shown in Figure 3d–f, and the relaxation times are given in Table I. Since there appears to be only a small contribution to basis spectra 2 and 3 from a deoxy-minus-CO spectrum, the fractional change in V_1 (the first column of the V matrix) gives a good first approximation to the change in fractional saturation with CO associated with each relaxation. These changes in fractional saturation are also given in Table I. The unnormalized spectra, $D_k(\lambda)$, calculated from eq 3 by using the fits of Figure 3 are shown

Table I: $1/e$ Times and Changes in Fractional Saturation Associated with Each Relaxation

hybrid	relaxation				
	I	II	III	IV	V
$\alpha(Co)_2\beta(Fe\text{-}CO)_2$					
$1/e$ times	76 ns	1.7 μs	27 μs	240 μs	6.5 ms
Δy[a]	0.37	0.05	0.12	0.23	0.24
	(0.35)	(0.03)	(0.09)	(0.25)	(0.28)
$\alpha(Fe\text{-}CO)_2\beta(Co)_2$					
$1/e$ times	53 ns	1.2 μs	15 μs	200 μs	7.7 ms
Δy	0.25	0.00	0.02	0.10	0.63
	(0.22)	(−0.02)	(0.00)	(0.10)	(0.70)
$\alpha(Fe\text{-}CO)_2\beta(Fe\text{-}CO)_2$					
$1/e$ times	57 ns	1.3 μs	20 μs	340 μs	6.3 ms
Δy	0.38	0.03	0.05	0.28	0.25
	(0.37)	(0.02)	(0.04)	(0.29)	(0.28)

[a] The values in parentheses were calculated from the first column of the V matrix (eq 2), while the values without parentheses were obtained after renormalization for the change in the deoxyheme spectra according to the procedure described by eq 6–8.

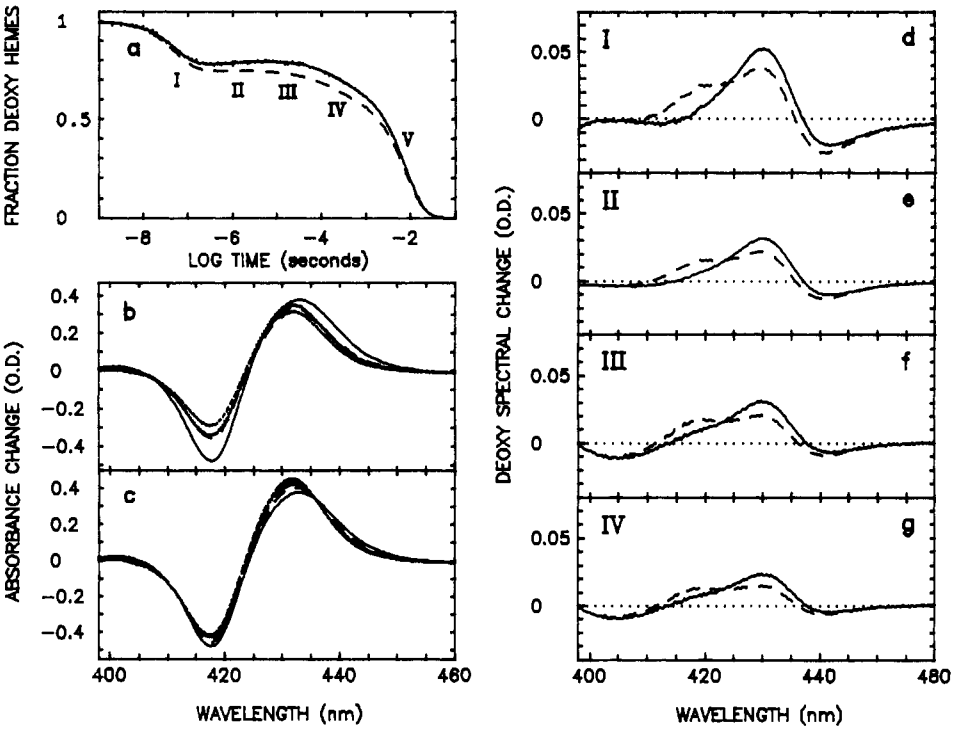

FIGURE 4: Ligand rebinding and spectral changes associated with each relaxation following photodissociation of $\alpha(\text{Fe-CO})_2\beta(\text{Co})_2$. (a) Ligand rebinding curve. The points are the first column of the V matrix, normalized to the maximum amplitude, and the solid curve is calculated from the result of the simultaneous least-squares fit to the first three columns of the V matrix in Figure 3d–f. The dashed curve is the corrected ligand rebinding curve calculated from the sum of five exponentials with relaxation times obtained from the fits to the first column of the V matrix (Table I) and amplitudes $([\text{Fe}]_{k+1} - [\text{Fe}]_k)/[\text{Fe}]_1$ calculated from the renormalization procedure described in the text (eq 6–8). (b) Spectra prior to each relaxation. (c) Spectra prior to each relaxation normalized to the spectrum prior to relaxation I by using the change in fractional saturation with CO calculated from the amplitudes of the fits to the first column of the V matrix. (d–g) Deoxyheme spectral changes associated with each relaxation. The dashed curves are the normalized difference spectra, $N_{k+1}(\lambda) - N_k(\lambda)$, and the solid curves are the renormalized spectra, $N^*_{k+1}(\lambda) - N^*_k(\lambda)$.

in Figure 4b. These spectra are simply the observed deoxy-minus-CO difference spectra prior to each of the five relaxations. The normalized spectra, $N_k(\lambda)$, calculated from eq 4 by using the fit to V_1 for normalization (Table I), are shown in Figure 4c. The spectral changes associated with each relaxation, $N_{k+1}(\lambda) - N_k(\lambda)$, are shown in Figure 4d–g. These spectral changes have extrema at the absorption maxima of HbCO (419 nm), indicating that the normalization for the concentration of deoxyhemes in eq 4 is not exact. There is also a small apparent decrease in the fractional saturation with CO in relaxation II (Figure 4a, Table I) that cannot result from CO dissociation, because it is much too fast. This result also indicates that there must be some error in treating V_1 as a ligand rebinding curve.

In order to minimize the contribution from ligand rebinding to the spectral changes accompanying each relaxation, the spectra were renormalized for the concentration of deoxyhemes by using an approximate method that takes into account the observed changes in the deoxyheme spectra. This renormalization procedure is described in detail under Materials and Methods (eq 6–8). It takes advantage of the fact that the changes in the deoxyheme spectrum are nearly an order of magnitude smaller than the average deoxy-minus-CO difference spectrum. The renormalization procedure produces physically sensible results for both the ligand rebinding curve and the deoxyheme spectral changes. Figure 4a and Table I compare the ligand rebinding curves obtained from V_1 and from renormalization for changes in the deoxyheme spectra. The apparent ligand dissociation is no longer present in relaxation II, and there is a significant increase in the amplitude of the geminate rebinding. Panels d–g of Figure 4 compare the spectra accompanying each relaxation before and after

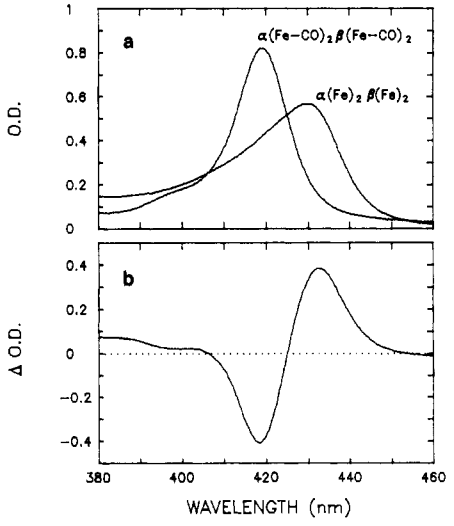

FIGURE 5: Static spectra of $\alpha(\text{Fe})_2\beta(\text{Fe})_2$ and $\alpha(\text{Fe-CO})_2\beta(\text{Fe-CO})_2$. (a) Absolute spectra of liganded (143 μM heme, path length = 343 μm) and unliganded unsubstituted hemoglobin (143 μM heme, path length = 342 μm). (b) Unliganded-minus-liganded difference spectrum.

renormalization. The comparison shows that the positive feature near the heme-CO peak has been largely suppressed as a result of the addition of a deoxy-minus-CO difference spectrum to the deoxyheme spectral change.

Comparable data sets were obtained for HbCO and for the hybrid molecule in which the iron in the α subunits was replaced by cobalt. Figure 5 shows the static spectra of Hb and HbCO; Figure 6 shows the results of singular-value decomposition; and Figure 7 shows the spectral changes accompa-

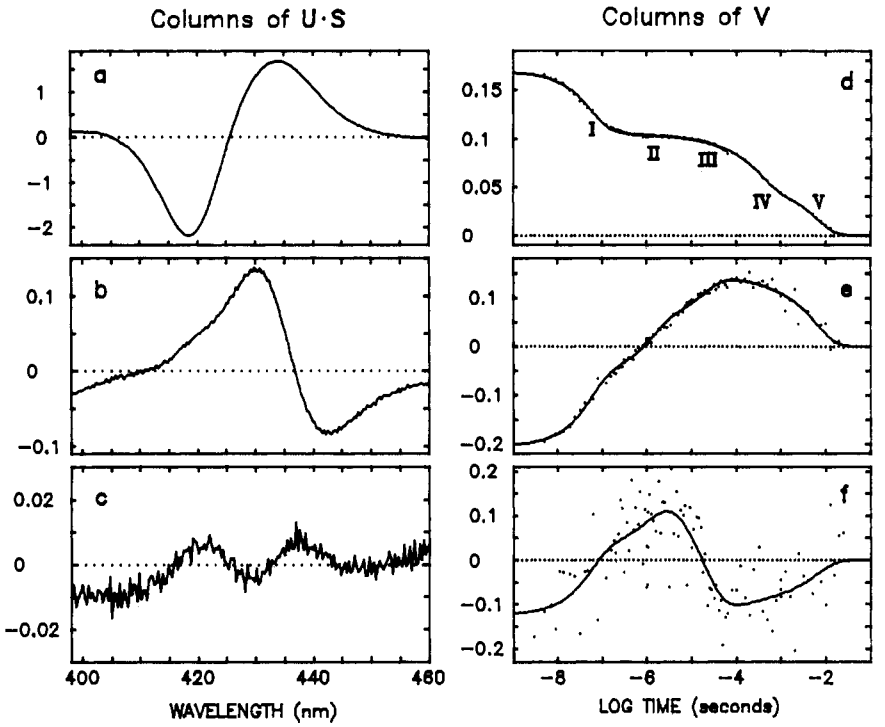

FIGURE 6: Singular-value decomposition of 102 spectra following photodissociation of α(Fe-CO)$_2\beta$(Fe-CO)$_2$ (sample of Figure 5). Panels a–c are the three significant basis spectra of the U matrix multiplied by their singular values. Panels d–f are the corresponding columns of the V matrix, which give the amplitude of the basis spectra as a function of time. The points are the data, and the solid curves are the results of simultaneous least-squares fits to the data using a sum of five exponentials (eq 2).

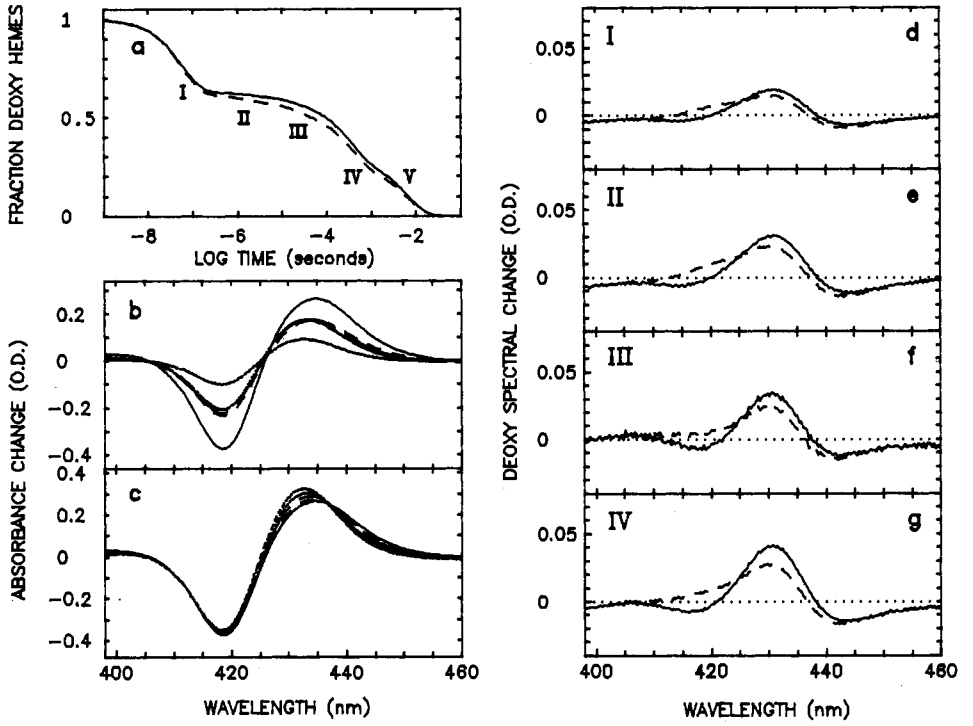

FIGURE 7: Ligand rebinding and spectral changes associated with each relaxation following photodissociation of α(Fe-CO)$_2\beta$(Fe-CO)$_2$. (a) Ligand rebinding curve. The points are the first column of the V matrix, normalized to the maximum amplitude, and the solid curve is calculated from the result of the simultaneous least-squares fit to the first three columns of the V matrix in Figure 6d–f. The dashed curve is the corrected ligand rebinding curve calculated from the sum of five exponentials with relaxation times obtained from the fits to the first column of the V matrix (Table I) and amplitudes $([Fe]_{k+1} - [Fe]_k)/[Fe]_1$ calculated from the renormalization procedure described in the text (eq 6–8). (b) Spectra prior to each relaxation. (c) Spectra prior to each relaxation normalized to the spectrum prior to relaxation I by using the change in fractional saturation with CO calculated from the amplitudes of the fits to the first column of the V matrix. (d–g) Deoxyheme spectral changes associated with each relaxation. The dashed curves are the normalized difference spectra, $N_{k+1}(\lambda) - N_k(\lambda)$, and the solid curves are the renormalized spectra, $N^*_{k+1}(\lambda) - N^*_k(\lambda)$.

nying each relaxation before and after renormalization. The corresponding results for α(Co)$_2\beta$(Fe-CO)$_2$ are shown in Figures 8, 9, and 10. For both molecules there were three significant basis spectra, and the columns of V were adequately fit with five exponentials, where the relaxation times in the independent and simultaneous fits were the same.

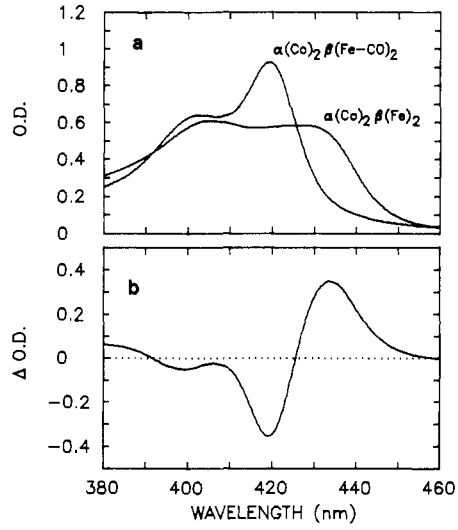

FIGURE 8: Static spectra of $\alpha(Co)_2\beta(Fe)_2$ and $\alpha(Co)_2\beta(Fe\text{-}CO)_2$. (a) Absolute spectra of liganded (128 μM heme, path length = 337 μm) and unliganded hybrid molecules (128 μM heme, path length = 337 μm). (b) Unliganded-minus-liganded difference spectrum.

The deoxyheme spectral changes for the iron–cobalt hybrids in Figures 4 and 10 show that below about 420 nm there are spectral changes that do not appear for R-state Hb (Figure 7) and are therefore assumed to arise from changes in the cobalt porphyrin absorption spectrum. The amplitudes of the cobalt porphyrin spectral changes are not correctly displayed in Figures 4 and 10 because they were obtained by normalizing the spectra to the concentration of deoxyhemes. To obtain the correct amplitudes, and to examine the changes in the cobalt porphyrin spectra more clearly, the contributions from ligand rebinding and deoxyheme spectral changes must be subtracted from the observed spectra. The problem is that the deoxyheme spectral changes for the cobalt-substituted molecules are not known separately, so we approximate these by the deoxyheme spectral changes observed for unsubstituted Hb. The change in the cobalt porphyrin spectrum associated with relaxation k, $[\Delta Co(\lambda)]_k$, is then given by

$$[\Delta Co(\lambda)]_k = [D_{k+1}(\lambda) - D_k(\lambda)] + \{D_1(\lambda)\Delta y_k + \Delta y_k \sum_{i=1}^{k} [\Delta Fe(\lambda)]_i\} - \{(1 - \sum_{i=1}^{k-1} \Delta y_i)[\Delta Fe(\lambda)]_k\} \quad (9)$$

where the $D_k(\lambda)$'s are the observed spectra prior to relaxation k, Δy_k is the change in fractional saturation with ligand accompanying relaxation k (Table I), and $[\Delta Fe(\lambda)]_k$ is the change in the deoxyheme spectrum in relaxation k. The first term in eq 9 is the difference in the observed spectra, the second term is the contribution to the observed difference from ligand rebinding, and the third term is the contribution from the change in the deoxyheme spectra. To evaluate $[\Delta Fe(\lambda)]_k$, the difference in the renormalized spectra for the hybrid, $N^*_{k+1}(\lambda) - N^*_k(\lambda)$, was fit between 420 and 440 nm with the difference spectrum from the corresponding relaxation for Hb by using the amplitude of the Hb difference spectrum and a wavelength shift as adjustable parameters. Because the deoxyheme spectral changes in Hb and the iron–cobalt hybrid are not identical, this procedure does not result in a "pure" cobalt porphyrin spectral change, but it provides a good first-order correction to the contribution of the deoxyheme spectral changes in the cobalt porphyrin absorption region.

It is clear from Figures 3, 6, and 9 that the use of five exponential relaxations provides a very good fit to the measured columns of V. Our data require five exponentials as a minimal representation but cannot preclude more complex models for the time evolution of the spectra. Comparison of fits to several independent data sets shows that the rates and changes in fractional saturation determined for the three processes, I, IV, and V, in which there is significant ligand rebinding are quite reproducible from experiment to experiment. The fitted rates

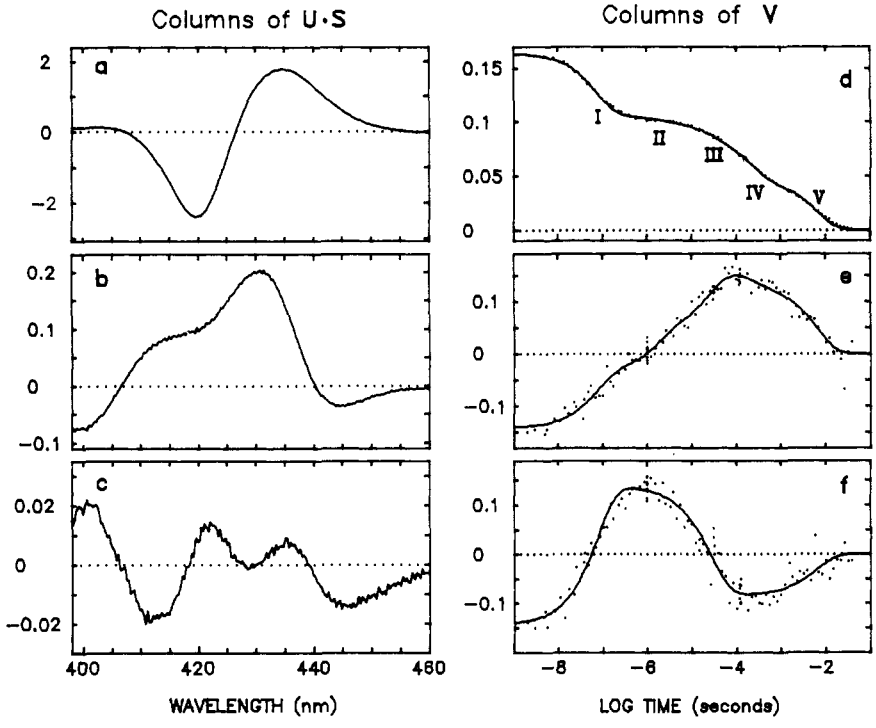

FIGURE 9: Singular-value decomposition of 107 spectra following photodissociation of $\alpha(Co)_2\beta(Fe\text{-}CO)_2$ (sample of Figure 8). Panels a–c are the three significant basis spectra of the U matrix multiplied by their singular values. Panels d–f are the corresponding columns of the V matrix, which give the amplitude of the basis spectra as a function of time. The points are the data, and the solid curves are the results of simultaneous least-squares fits to the data using a sum of five exponentials (eq 2).

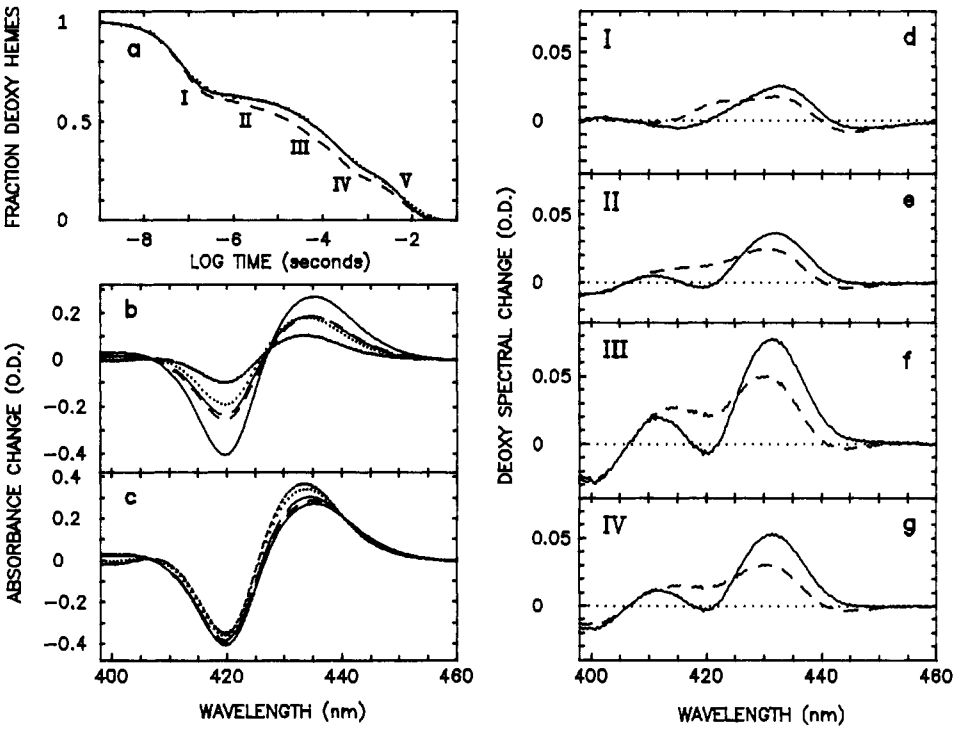

FIGURE 10: Ligand rebinding and spectral changes associated with each relaxation following photodissociation of $\alpha(Co)_2\beta(Fe\text{-}CO)_2$. (a) Ligand rebinding curve. The points are the first column of the V matrix, normalized to the maximum amplitude, and the solid curve is the result of the simultaneous least-squares fit to the first three columns of the V matrix in Figure 9d–f. The dashed curve is the corrected ligand rebinding curve calculated from the sum of five exponentials with relaxation times obtained from the fits to the first column of the V matrix (Table I) and amplitudes $([Fe]_{k+1} - [Fe]_k)/[Fe]_1$ calculated from the renormalization procedure described in the text (eq 6–8). (b) Spectra prior to each relaxation. (c) Spectra prior to each relaxation normalized to the spectrum prior to relaxation I by using the change in fractional saturation with CO calculated from the amplitudes of the fits to the first column of the V matrix. (d–g) Deoxyheme spectral changes associated with each relaxation. The dashed curves are the normalized difference spectra, $N_{k+1}(\lambda) - N_k(\lambda)$, and the solid curves are the renormalized spectra, $N^*_{k+1}(\lambda) - N^*_k(\lambda)$.

agree to within ±20% and the Δy values to within ±1%. On the other hand, the rates of the processes that are primarily spectral changes (II and III) are less well determined. The error in the determination of these rates is at least ±50%. This error becomes important in comparing the magnitudes of the spectral changes associated with each relaxation. Because V_2 increases monotonically with time during the intermediate portion of each experiment, an increase in the values of k_{II} and k_{III} borrows intensity for the spectral changes from relaxation I, while a decrease in these two rates borrows intensity from relaxation IV. The uncertainty in the rates for these processes generates a correspondingly large uncertainty (±30%) in the amplitudes of the spectral changes associated with relaxations I–IV.

Figures 11 and 12 summarize the major results for all three molecules, showing the ligand rebinding curve, the deoxyheme spectral changes, and the cobalt porphyrin spectral changes.

Discussion

In this study we have measured the Soret absorption spectra between 0 and about 50 ms following complete photodissociation of the $\alpha(Co)_2\beta(Fe\text{-}CO)_2$ and $\alpha(Fe\text{-}CO)_2\beta(Co)_2$ hybrid hemoglobin molecules and compared the results with those found for HbCO, i.e., $\alpha(Fe\text{-}CO)_2\beta(Fe\text{-}CO)_2$. After the data were processed by singular-value decomposition and least-squares fitting to the relaxation curves, three major results were obtained for each molecule: the ligand rebinding curve and spectral changes accompanying each of the observed relaxations, which are shown in Figures 11 and 12, and the relaxation times, given in Table I. As in the case of HbCO, five exponential relaxations were observed for each molecule (Hofrichter et al., 1983). To interpret these data, it is important to have some kinetic model as a working hypothesis. For this purpose we shall use, as before, the framework of the two-state allosteric model, which assumes that there are only two types of kinetic behavior, one for subunits in the R quaternary structure and one for subunits in the T quaternary structure (Hopfield et al., 1971; Sawicki & Gibson, 1976). It is important at the outset, then, to know the quaternary structure of the liganded and unliganded molecules at equilibrium. To obtain an independent determination of the quaternary structure of the liganded hybrids, it is necessary to extrapolate from the results of experiments under a variety of solution conditions, since the liganded hybrids have not been studied under the conditions of our experiments (0.1 M potassium phosphate and 0.01 M sodium dithionite, pH 7.0, 20–22 °C). We discuss first the hybrid in which the iron of both α subunits has been replaced by cobalt.

There is both spectroscopic and kinetic data to indicate that the unliganded hybrid, $\alpha(Co)_2\beta(Fe)_2$, is in the T state. In 0.1 M potassium phosphate, pH 7.0, at 20 °C, CO binds with the characteristically slow bimolecular rate constant of the T state (1×10^5 M^{-1} s^{-1}) and exhibits no fast rebinding phase (Ikeda-Saito & Yonetani, 1980). Proton magnetic resonance measurements indicate that the intersubunit hydrogen bonds of the T state are intact for the unliganded hybrid in 0.05 M [bis(2-hydroxyethyl)amino]tris(hydroxymethyl)methane (Bis-Tris) buffer, pH 7.0, at 23 °C (T. Inubushi and T. Yonetani, unpublished results). The oxygen affinity of the cobalt porphyrins in the liganded hybrid, $\alpha(Co)_2\beta(Fe\text{-}CO)_2$, in 0.05 M Bis-Tris buffer, pH 7.0, at 15 °C, with and without IHP, is comparable to that found in an R-state hemoglobin in which all four iron atoms have been replaced by cobalt (Ikeda-Saito & Yonetani, 1980). Proton magnetic resonance experiments

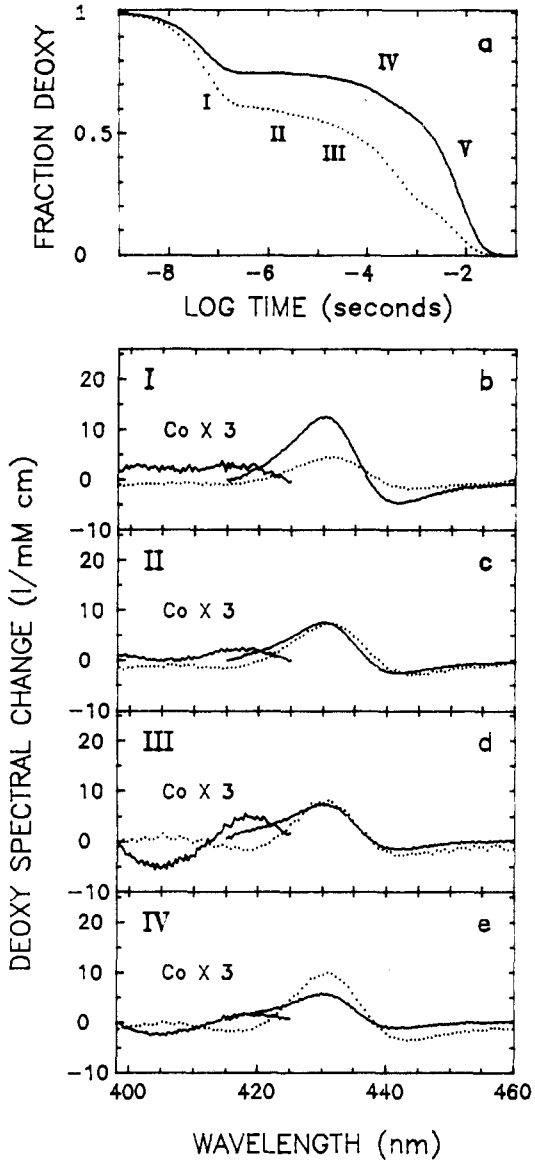

FIGURE 11: Corrected ligand rebinding curve, deoxyheme spectral changes, and cobalt porphyrin spectral changes following photodissociation of $\alpha(\text{Fe-CO})_2\beta(\text{Co})_2$ and $\alpha(\text{Fe-CO})_2\beta(\text{Fe-CO})_2$. (a) Corrected ligand rebinding curves for the hybrid molecule (solid curve, same as dashed curve in Figure 4a) and for R-state Hb (dotted curve, same as dashed curve in Figure 7a). (b–e) Deoxyheme and cobalt porphyrin spectral changes accompanying each of the first four relaxations. The dotted curves are for R-state Hb. The solid curves between 415 and 460 nm are the deoxyheme spectral changes for the hybrid molecule, and the solid curves between 398 and 425 nm are the cobalt porphyrin spectral changes for the hybrid molecule calculated from eq 9. The deoxyheme spectral changes are $[N^*_{k+1}(\lambda) - N^*_k(\lambda)]/cl$, where c is the concentration of hemes and l is the path length, and the cobalt porphyrin spectral changes are $[\Delta\text{Co}(\lambda)]_k/cl$, where c is the concentration of cobalt porphyrins (eq 9). The cobalt porphyrin spectral changes have been multiplied by a factor of 3.

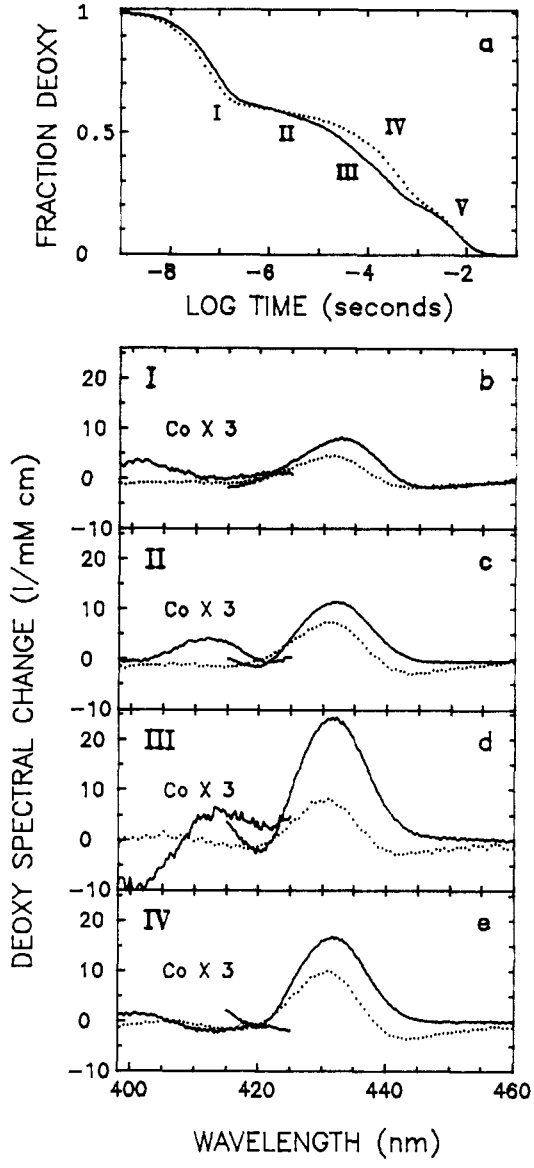

FIGURE 12: Corrected ligand rebinding curve, deoxyheme spectral changes, and cobalt porphyrin spectral changes following photodissociation of $\alpha(\text{Co})_2\beta(\text{Fe-CO})_2$ and $\alpha(\text{Fe-CO})_2\beta(\text{Fe-CO})_2$. (a) Corrected ligand rebinding curves for the hybrid molecule (solid curve, same as dashed curve in Figure 10a) and for R-state Hb (dotted curve, same as dashed curve in Figure 7a). (b–e) Deoxyheme and cobalt porphyrin spectral changes accompanying each of the first four relaxations. The dotted curves are for R-state Hb. The solid curves between 415 and 460 nm are the deoxyheme spectral changes for the hybrid molecule, and the solid curves between 398 and 425 nm are the cobalt porphyrin spectral changes for the hybrid molecule calculated from eq 9. The deoxyheme spectral changes are $[N^*_{k+1}(\lambda) - N^*_k(\lambda)]/cl$, where c is the concentration of hemes and l is the path length, and the cobalt porphyrin spectral changes are $[\Delta\text{Co}(\lambda)]_k/cl$, where c is the concentration of cobalt porphyrins (eq 9). The cobalt porphyrin spectral changes have been multiplied by a factor of 3.

are consistent with this conclusion. Measurements in the hydrogen-bonding region indicate that the intersubunit hydrogen bonds of $\alpha(\text{Co})_2\beta(\text{Fe-CO})_2$ are broken upon binding of CO to the hemes in 0.05 M Bis-Tris buffer, pH 7.0, at 23 °C in the presence and absence of inositol hexaphosphate (IHP) (T. Inubushi and T. Yonetani, unpublished results). Furthermore, resonance Raman studies of the immediate photoproduct of photolysis with 10-ns pulses at 35 °C with IHP show an iron–histidine stretching frequency characteristic of the R state (Scott et al., 1983). We assume at the outset, then, that under our conditions all $\alpha(\text{Co})_2\beta(\text{Fe-CO})_2$ molecules are in the R quaternary state prior to photolysis and that the fully unliganded molecule will eventually convert to the T state.

Following photodissociation of $\alpha(\text{Co})_2\beta(\text{Fe-CO})_2$ both the ligand rebinding curve and spectral changes in the deoxyheme absorption region are very similar to those found for photodissociation of R-state HbCO (Figure 12). The bulk of the bimolecular ligand rebinding takes place at times greater than about 50 μs, and, as for R-state HbCO, is biphasic (relaxations IV and V). This biphasic behavior has been previously interpreted as resulting from bimolecular rebinding to molecules in the R quaternary structure followed by rebinding to mol-

ecules in the T quaternary structure, which have switched from R to T before and during the R-state rebinding phase (Sawicki & Gibson, 1976; Hofrichter et al., 1983). The amplitude of the slow rebinding phase is similar for the hybrid and Hb. Since the lower *total* saturation of the hybrid (which has only two binding sites) would be expected to favor formation of T-state molecules, this result supports the initial assumption that all $\alpha(Co)_2\beta(Fe\text{-}CO)_2$ molecules are in the R quaternary structure.

The geminate yield in relaxation I for the hybrid molecule is 0.37, which is the same as that found for R-state HbCO (Table I). The relaxation time for the geminate process is 76 ns, compared to 57 ns for R-state HbCO. The near identity of the geminate phases (relaxation I) after complete photodissociation suggests that both the geminate yield and relaxation time of the α and β subunits in the R-state Hb tetramer are very similar.

Comparison of the spectral changes accompanying each relaxation after photolysis of $\alpha(Co)_2\beta(Fe\text{-}CO)_2$ suggests that the α and β hemes also make comparable contributions to the spectral changes in R-state Hb. Panels b–e of Figure 12 compare the spectral changes accompanying each of the first four relaxations. The spectral changes have very similar shapes between 420 and 460 nm, where changes in the deoxyheme spectra are expected.

As was found for R-state Hb, there is a spectral change of the deoxyhemes associated with relaxation I. This finding for the hybrid eliminates the possibility raised in the Hb study (Hofrichter et al., 1983) that the spectral change in R-state Hb for relaxation I may not reflect a conformational change but may result from unequal geminate recombination to α and β subunits that have different absorption spectra.

Relaxations II–IV also show spectral changes in the deoxyheme absorption region that are similar to those observed for R-state Hb. The $1/e$ times for relaxations II and III are 1.7 and 27 μs, respectively, compared to 1.3 and 20 μs, respectively, for R-state Hb. The similarity in the relaxation times and the shape of the spectral changes suggests that they correspond to the same processes observed for R-state Hb, in which relaxation II was interpreted as a tertiary conformational change and relaxation III as the quaternary conformational change for zero-liganded molecules (Hofrichter et al., 1983). On the assumption of statistical rebinding of CO in relaxations I and II, about 15% of the deoxyhemes are predicted to switch from R to T in relaxation III for R-state Hb, while about 50% of the deoxyhemes in the hybrid sample are predicted to switch. This calculation suggests that the amplitude of the deoxyheme spectral change in Figure 12d should be about 3 times larger for the hybrid molecule compared to R-state Hb, which is close to the observed ratio of the amplitudes.[2]

The spectral change associated with relaxation IV also looks very much like the T-minus-R difference spectrum of relaxation III. Since the species rebinding CO in relaxation V does so with a T-state binding rate, we assume that all R-state deoxyhemes have disappeared by the end of relaxation IV, either by rebinding CO or by switching from R to T. The magnitude of the deoxyheme spectral change in relaxation IV is close to what was found for relaxation III. This is consistent with the estimate that 50% of the deoxyhemes are in R-state molecules prior to relaxation IV and that all the deoxyhemes remaining after relaxation IV are in T-state molecules.

[2] The T-minus-R difference spectrum for unsubstituted Hb reported here is similar to that measured by Sawicki & Gibson (1976) in the region 425–460 nm. There are, however, significant differences in the region 410–425 nm, for which there is no obvious explanation.

A novel aspect of these experiments is that we can utilize the cobalt porphyrin absorption region to observe the response of the cobalt-containing α subunits to the photodissociation of CO in the iron-containing β subunits. An important negative result is that for relaxation I there is no significant spectral change at wavelengths shorter than 415 nm (Figure 12b), where the cobalt porphyrin shows a clear spectral change in the static difference spectrum from CO binding to the hemes (Figure 8). Relaxations II and III, on the other hand, show spectral changes in the cobalt porphyrin region. These are similar to the change observed in the static difference spectrum (Figure 8), which exhibits a negative peak at about 400 nm. The change in the cobalt porphyrin spectrum in relaxation III is expected since the R $\rightarrow$ T quaternary change produces conformational changes in all four subunits (Perutz, 1970; Baldwin & Chothia, 1979). The absence of a similar spectral change in relaxation IV indicates that there is no significant switching from R to T of singly liganded molecules.

Since no change is observed in the cobalt porphyrin region in relaxation I, we may conclude that the structure of the α subunit is not changed by photodissociation of CO in the β subunit until relaxation II at 1.7 μs. This result is consistent with the previous result on R-state Hb, where it was found that the geminate yield and $1/e$ time of relaxation I were the same for molecules that were fully photodissociated and 22% photodissociated (Hofrichter et al., 1983). Even though most of the molecules in the partial photolysis experiment remain either doubly or triply liganded after photolysis, the deoxy subunits showed the same geminate kinetics as the deoxy subunits in which all of the molecules were completely unliganded.

The unexpected result is that there is a small change in the spectrum of the cobalt porphyrins associated with relaxation II. If our assignment of relaxation II is correct, the cobalt porphyrin spectral change results from the propagation of tertiary conformational changes from the photolyzed β subunit to the α subunit, without a change in quaternary structure. The tertiary conformational change in the α subunit could reflect a slow response of the α subunit to the photodissociation event or to relaxation I in the β subunit, or it could be a much more rapid response to the tertiary conformational change of relaxation II in the β subunit. It is not possible from the present data to draw any more detailed conclusions concerning the temporal relation between the tertiary changes in the α and β subunits. The time course of the cobalt porphyrin spectrum cannot be observed independently, because there is no wavelength in the Soret region where the cobalt porphyrin spectrum can be observed without interference from the ligand rebinding or deoxyheme spectral changes. For the present, then, we can only conclude that the cobalt porphyrin spectral change takes place at about 1 μs and is simultaneous with the deoxyheme spectral change.

We now turn to the results for the hybrid molecule in which the iron of the β hemes has been replaced by cobalt. Spectroscopic and kinetic data suggest that the unliganded molecule, $\alpha(Fe)_2\beta(Co)_2$, is in the T quaternary structure. Proton magnetic resonance data show that the intersubunit hydrogen bonds in 0.05 M Bis-Tris buffer, pH 7.0, at 23 °C are intact. In stopped-flow kinetic experiments CO binds with a slow rate of 6.4×10^4 M^{-1} s^{-1} in 0.1 M potassium phosphate at 20 °C, and no fast phase is observed (Ikeda-Saito & Yonetani, 1980; Blough et al., 1980). The quaternary structure of the liganded form, $\alpha(Fe\text{-}CO)_2\beta(Co)_2$, appears to depend on solution conditions. In transient resonance Raman experiments at 35 °C in the presence of IHP the iron–histidine stretching frequency

of the immediate photoproduct of photolysis with 10-ns laser pulses is similar to what is found for T-state molecules (Scott et al., 1983). At 15 °C in 0.05 M Bis-Tris buffer the oxygen affinity of the cobalt porphyrins is similar to that found for R-state cobalt porphyrins, but on the addition of IHP the affinity decreases about 8-fold, suggesting that most of the molecules have switched to the T state (Ikeda-Saito & Yonetani, 1980). This is qualitatively consistent with proton magnetic resonance data, which suggest that the intersubunit bonds are absent in 0.05 M Bis-Tris buffer, pH 7.0, at 23 °C and form upon the addition of IHP (Inubushi & Yonetani, unpublished results).

The oxygen binding and spectroscopic data would suggest, then, that under the conditions of our experiment both R and T states of $\alpha(\text{Fe-CO})_2\beta(\text{Co})_2$ are significantly populated. This is also suggested by the ligand rebinding curve and spectral changes that we observe after photodissociation (Figures 10 and 11). The slow phase of the bimolecular rebinding (Figure 11a) is about 90% of the total amplitude for bimolecular rebinding, which is most easily interpreted as arising from a significant fraction of T-state molecules prior to photolysis. The results for both the geminate rebinding and R → T spectral changes are consistent with this conclusion. The geminate yield for relaxation I is 0.25, and the $1/e$ time is 53 ns (Table I). These parameters are very similar to those observed for photodissociation of hemoglobin that was initially 10% saturated with CO (0.21 and 45 ns), in which it was estimated that about 65% of the liganded hemes prior to photolysis were in T-state molecules (Hofrichter et al., 1983). The spectral data also suggest that $\alpha(\text{Fe-CO})_2\beta(\text{Co})_2$ is partially in the T state. We interpret the spectral change of relaxation III at 15 μs as arising from the R → T transition for the unliganded molecules. The amplitude of this change is similar to that of R-state Hb and much smaller than the change observed for $\alpha(\text{Co})_2\beta(\text{Fe-CO})_2$ (Figure 12d), suggesting that less than half of the zero-liganded molecules undergo an R → T transition. An important consequence of this interpretation is that the lower geminate yield for $\alpha(\text{Fe-CO})_2\beta(\text{Co})_2$ compared to that for $\alpha(\text{Co})_2\beta(\text{Fe-CO})_2$ is explained by the presence of a significant fraction of T-state molecules with a low (<0.2) geminate yield and does not result from a lower geminate yield for α subunits compared to β subunits in the R state. For example, if 50% of the hemes were in R-state molecules prior to photolysis with a geminate yield of 0.38, the observed yield of 0.25 would result from a T-state yield of 0.12.

The deoxyheme spectral changes in the $\alpha(\text{Fe-CO})_2\beta(\text{Co})_2$ hybrid are similar to those for the $\alpha(\text{Co})_2\beta(\text{Fe-CO})_2$ hybrid (Figure 11b–e). There are, however, several significant differences. In addition to the difference in the amplitude of the spectral change in the R → T transition at 15 μs discussed above, the amplitude of the spectral change accompanying geminate rebinding in relaxation I is much larger than that observed for either $\alpha(\text{Co})_2\beta(\text{Fe-CO})_2$ or R-state Hb. A large part of this difference could be accounted for by preferential geminate rebinding to R-state molecules, for which the immediate photoproduct has a different spectrum from that of T-state molecules (Hofrichter et al., 1983). In contrast, the spectral change of relaxation II is similar in all three molecules. The similarity of both the $1/e$ times and the spectral amplitudes for relaxation II in $\alpha(\text{Fe-CO})_2\beta(\text{Co})_2$ compared to $\alpha(\text{Co})_2\beta(\text{Fe-CO})_2$ and R-state Hb (Table I) implies that the relaxation time and spectral change for this tertiary conformational change are similar for the R and T quaternary structures.

The cobalt porphyrin spectrum of the β subunit responds to photodissociation of CO in the α subunits. Unlike the cobalt porphyrin spectral change for the $\alpha(\text{Co})_2\beta(\text{Fe-CO})_2$ hybrid, the cobalt porphyrin spectral change for the $\alpha(\text{Fe-CO})_2\beta(\text{Co})_2$ hybrid is not the same as that found in the static difference spectrum. The static difference spectrum, $\alpha(\text{Fe})_2\beta(\text{Co})_2$ minus $\alpha(\text{Fe-CO})_2\beta(\text{Co})_2$, in Figure 1b does not show any feature in the cobalt porphyrin absorption region that is significantly different than what is observed for Hb (Figure 5b). In the transient spectra, however, there are negative and positive extrema at 405 and 418 nm, respectively, associated with relaxations II–IV, which we interpret as arising from a change in the cobalt porphyrin spectrum. This change is similar to the cobalt porphyrin spectral change observed in the transient spectra following photodissociation of $\alpha(\text{Co})_2\beta(\text{Fe-CO})_2$ but is red shifted by about 5 nm, and it could therefore be easily obscured in the static difference spectra in Figure 1b. As in the case of the $\alpha(\text{Co})_2\beta(\text{Fe-CO})_2$ hybrid, there is no change in the cobalt porphyrin spectrum during relaxation I, a small change is observed in relaxation II, and a much larger change is observed in relaxation III, the R → T quaternary transition. Unlike the $\alpha(\text{Co})_2\beta(\text{Fe-CO})_2$ hybrid, a cobalt porphyrin spectral change is observed in relaxation IV, indicating that singly liganded R-state molecules switch to T during this relaxation. This is consistent with the equilibrium studies, which suggest that the T state is more favored in singly liganded $\alpha(\text{Fe-CO})\alpha(\text{Fe})\beta(\text{Co})_2$ compared to singly liganded $\alpha(\text{Co})_2\beta(\text{Fe-CO})\beta(\text{Fe})$.

It is useful to briefly compare the results on the iron–cobalt hybrid hemoglobins with those of the isolated subunits, which have been examined by single-wavelength kinetic studies in the Soret region (Lindqvist et al., 1980, 1981). In these experiments the geminate yield was about one-third lower for both the isolated α and isolated β subunits than for R-state Hb (Lindqvist et al., 1981), whereas we have observed the same geminate yield for the $\alpha(\text{Co})_2\beta(\text{Fe-CO})_2$ hybrid and R-state Hb. Further, the isolated subunits exhibited smaller spectral changes than were observed for R-state Hb (Lindqvist et al., 1980). It would appear that the isolated subunits have significantly different spectral and kinetic properties than the subunits in the intact R-state tetramer, as judged by the results on the iron–cobalt hybrids.

Finally, we should point out that a major outstanding problem in the recent nanosecond photodissociation work on hemoglobin is the determination of the nature of the tertiary conformational changes in relaxations I and II and their relation to the motion of the ligand in the protein. Unfortunately, these results on the iron–cobalt hybrids do not help distinguish among models for the conformational changes. There appear to be two extreme models for the tertiary conformational changes that have very different consequences for the overall kinetic mechanism. In the first model the conformational changes are an effectively instantaneous response of the globin to the motion of CO from one part of the protein to another (relaxation I) and from the protein into the solvent (relaxation II). This model has two virtues. It implies a kinetic mechanism in which the dissociation and association pathways are the same, so that all of the rate constants of the mechanism can be calculated from the relaxation times of the photolysis experiment and the overall dissociation and association rates (Hofrichter et al., 1983; Henry et al., 1984). This is a sequential barrier model (Austin et al., 1975), with the addition of conformational changes that are a passive response to the ligand motion. A second model postulates that the conformational changes are the response of the molecule to photo-

dissociation and not to the location of CO in the protein. In this case the conformational changes can alter the rate at which CO rebinds to the heme or moves inside the protein; if the conformational changes are slow relative to these processes, the dissociation and association paths can be different. The immediate photoproduct could then be an intermediate in the thermal dissociation pathway but not be a significant intermediate in the association pathway because CO entering from the solvent would encounter a different protein structure. This mechanism is more complex, and it is not possible to obtain the rate constants for the individual steps of the association pathway from the existing experimental data.

Conclusions

From this limited study of iron–cobalt hybrid hemoglobins we have obtained important new experimental information on two aspects of the problem of understanding the processes that occur subsequent to photodissociation of CO. First, we have been able to assess the relative contributions of the α and β subunits to both the geminate recombination and spectral changes of the deoxy subunits in the R-state tetramer. Second, we have observed the time-resolved response of the α subunits to photodissociation in the β subunits, and vice versa.

Because the geminate yield and relaxation time are so similar for photodissociation of the $\alpha(Co)_2\beta(Fe\text{-}CO)_2$ hybrid, compared to R-state HbCO, we have concluded that the α and β subunits in R-state Hb have approximately equal geminate yields and recombination times. The results for the $\alpha(Fe\text{-}CO)_2\beta(Co)_2$ hybrid are consistent with this conclusion, even though the analysis for this molecule is complicated by the presence of comparable populations of R- and T-state species.

Although the spectral changes for the deoxyhemes in the two hybrids are slightly different, it is clear that both subunits make roughly equal contributions to the spectral changes observed in the R-state tetramer, which reflect tertiary and quaternary conformational changes. The response of the cobalt porphyrins to photodissociation is similar in the two hybrids. No structural change is detected in the cobalt-containing subunits until the second tertiary conformational change in the iron-containing subunits, observed at 1–2 μs. A much larger structural change, as judged by the amplitude of the spectral changes, takes place in the cobalt-containing subunits concomitant with the R $\rightarrow$ T quaternary change at about 20 μs.

Because both R- and T-state molecules contribute to the properties of the $\alpha(Fe\text{-}CO)_2\beta(Co)_2$ hybrid, it will be important in future studies to simplify the analysis by working with a single quaternary structure.

Registry No. CO, 630-08-0.

References

Alpert, B., El Mohsni, S., Lindqvist, L., & Tfibel, F. (1979) *Chem. Phys. Lett. 64*, 11–16.

Austin, R. H., Beeson, K. W., Eisenstein, L., Frauenfelder, H., & Gunsalus, I. C. (1975) *Biochemistry 14*, 5355–5373.

Baldwin, J. M., & Chothia, C. (1979) *J. Mol. Biol. 129*, 175–220.

Blough, N. V., Zemel, H., Hoffman, B. M., Lee, T. C. K., & Gibson, Q. H. (1980) *J. Am. Chem. Soc. 102*, 5683–5685.

Catterall, R., Duddell, D. A., Morris, R. J., & Richards, J. T. (1982) *Biochim. Biophys. Acta 705*, 256–263.

Duddell, D. A., Morris, R. J., & Richards, J. T. (1979) *J. Chem. Soc., Chem. Commun.*, 75–76.

Fermi, G., Perutz, M. F., Dickinson, L. C., & Chien, J. C. W. (1982) *J. Mol. Biol. 155*, 495–505.

Friedman, J. M., & Lyons, K. B. (1980) *Nature (London) 284*, 570–573.

Friedman, J. M., Rousseau, D. L., & Ondrias, M. R. (1982) *Annu. Rev. Phys. Chem. 33*, 471–491.

Golub, G. H., & Reinsch, C. (1970) *Numer. Math. 14*, 403–420.

Henry, E. R., Sommer, J. H., Hofrichter, J., & Eaton, W. A. (1983) *J. Mol. Biol. 166*, 443–451.

Henry, E. R., Hofrichter, J., Sommer, J. H., & Eaton, W. A. (1984) in *Photochemistry and Photobiology* (Zewail, A. W., Ed.) Vol. 2, pp 791–810, Harwood, New York.

Ho, C., Eaton, W. A., Collman, J. P., Gibson, Q. H., Leigh, J. S., Margoliash, E., Moffatt, J. K., & Scheidt, W. R., Eds. (1982) *Hemoglobin and Oxygen Binding*, pp 322–467, Elsevier/North-Holland, Amsterdam.

Hofrichter, J., Sommer, J. H., Henry, E. R., & Eaton, W. A. (1983) *Proc. Natl. Acad. Sci. U.S.A. 80*, 2235–2239.

Hopfield, J. J., Shulman, R. G., & Ogawa, S. (1971) *J. Mol. Biol. 61*, 425–443.

Ikeda-Saito, M., & Yonetani, T. (1980) *J. Mol. Biol. 138*, 845–858.

Ikeda-Saito, M., Yamamoto, H., & Yonetani, T. (1977) *J. Biol. Chem. 252*, 8639–8644.

Imai, K., Yonetani, T., & Ikeda-Saito, M. (1977) *J. Mol. Biol. 109*, 83–97.

Lindqvist, L., El Mohsni, S., Tfibel, F., & Alpert, B. (1980) *Nature (London) 288*, 729–730.

Lindqvist, L., El Mohsni, S., Tfibel, F., Alpert, B., & Andre, J. C. (1981) *Chem. Phys. Lett. 79*, 525–528.

Lyons, K. B., & Friedman, J. M. (1982) in *Hemoglobin and Oxygen Binding* (Ho, C., Eaton, W. A., Collman, J. P., Gibson, Q. H., Leigh, J. S., Margoliash, E., Moffat, J. K., and Scheidt, W. R., Eds.) pp 333–338, Elsevier/North-Holland, Amsterdam.

Morris, R. J., Gibson, Q. H., Ikeda-Saito, M., & Yonetani, T. (1984) *J. Biol. Chem. 259*, 6701–6703.

Noe, L. J. (1982) in *Biological Events Probed by Ultrafast Laser Spectroscopy* (Alfano, R. R., Ed.) pp 339–357, Academic Press, New York.

Perutz, M. F. (1970) *Nature (London) 228*, 726–734.

Sawicki, C. A., & Gibson, Q. H. (1976) *J. Biol. Chem. 251*, 1533–1542.

Scott, T. W., Friedman, J. M., Ikeda-Saito, M., & Yonetani, T. (1983) *FEBS Lett. 158*, 68–72.

Shrager, R. I., & Hendler, R. W. (1982) *Anal. Chem. 54*, 1147–1152.

Sunshine, H. R., Hofrichter, J., & Eaton, W. A. (1979) *J. Mol. Biol. 133*, 435–467.